Desalination and Water Treatment
www.deswater.com

doi: 10.5004/dwt.2019.23506

142 (2019) 140–147
February

Treatment of real petroleum refinery wastewater with alternative ferrous-assisted UV/persulfate homogeneous processes

Omid Pourehie, Javad Saien*

Department of Applied Chemistry, Bu-Ali Sina University, Hamedan 65174, Iran, Tel. +98 81 38282807; emails: saien@basu.ac.ir (J. Saien), omidpourehie@gmail.com (O. Pourehie)

Received 11 May 2018; Accepted 21 November 2018

ABSTRACT

Treatment of real refinery wastewater was investigated based on alternative ferrous-assisted ultraviolet/persulfate (UV/PS/Fe^{2+}) homogeneous processes. An effective circulating photo-reactor, equipped with an only 6 W, UV lamp was employed. The effects of operating parameters, including PS salt and ferrous sulfate salt (to supply ferrous ion) dosages, solution pH, reaction time, temperature, and applying ultrasound (US) waves were studied. The criteria in degradation process were the chemical oxygen demand (COD) and the total organic carbon (TOC). The optimum operating conditions were found at PS concentration of 302.9 mg L^{-1}, ferrous sulfate salt concentration of 20.3 mg L^{-1} and pH of 4.8, under which the COD, turbidity, and TOC of the wastewater were reduced respectively to 66.6%, 76.9%, and 39.2% after 60 min. Increasing temperature from 25°C to 50°C and applying US caused significant enhancements in these criteria. From results, the efficiency of investigated processes was appeared in the order of UV/PS/Fe^{2+}/US > UV/PS/Fe^{2+}/heat > UV/PS/Fe^{2+} > UV/PS > UV. An overall first-order rate of COD removal was detected for the UV/PS/Fe^{2+} process and accordingly, the electrical energy consumption for one order of magnitude COD removal, under optimum conditions, was 10.56 kWh m^{-3} as well as total operating cost of only \$1.82 m^{-3}.

Keywords: Refinery wastewater; UV/persulfate; Ferrous ion; Ultrasonic waves; Cost estimation

1. Introduction

Recently, a high interest has been devoted to petroleum refinery with the aim of wastewater management by optimizing water consumption and employing treating techniques to reuse the treated wastewater. The traditional treatment of petroleum refinery wastewater is based on physical and chemical methods and further biological treatments in the integrated activate sludge unit. With respect to the fact that significant aliphatic and aromatic petroleum hydrocarbons exist in refinery wastewaters, among which aromatics are not readily degradable, there is still needs to use advanced techniques to remove these pollutants as much as possible [1].

During recent decades, use of peroxysulfates has gained much attention for water and wastewater treatments [2,3]. In many studies it has been shown that they are capable of degrading highly toxic and persistent pollutants and are relatively cheap in comparison to other oxidants. Persulfate (PS) ion ($S_2O_8^{2-}$) utilizing with either radical driven or direct electron transfer process is a powerful method for treatment of a broad range of impurities including halogenated olefins and benzene, toluene, ethylbenzene and xylenes [4,5]. PS salts are very stable in the solid state and another advantage of these salts, in comparison to other reagents (hydrogen peroxide or ozone), is their safety and low transportation issues [6]. In a study by Babaei and Ghanbari in treatment of a petrochemical real wastewater, the performance of PS has been compared with hydrogen peroxide and percarbonate, all activated with ultraviolet (UV) irradiation [7].

When PS ion is activated in aqueous media, it forms sulfate anion radical ($SO_4^{\bullet-}$) with a high oxidation potential

* Corresponding author.

of 2.5–3.1 V [8] and with a kinetically fast reacting with organic pollutants in wastewaters. PS can be activated by heat [9], UV light [10], carbon catalyst [11], soil minerals [12], radiolysis [13] as well as transition metal ions [14,15] to form sulfate radicals. Degradation of pollutants is extremely dependent on the PS activation technique. Sulfate radical based advanced oxidation processes (AOPs) has recently drawn much attention as one suitable in situ chemical oxidation technique [16].

Exposure to UV radiation is one effective PS activation. It has been demonstrated experimentally that photolysis of PS results in cleavage of the peroxide bonds and formation of two sulfate anion radicals. Briefly, generation of the radicals in aqueous media has been described via the following reactions [17,18]:

$$S_2O_8^{2-} \xrightarrow{hv} 2SO_4^{\bullet-} \quad (1)$$

$$SO_4^{\bullet-} + H_2O \rightarrow SO_4^{2-} + HO^{\bullet} + H^+ \quad (2)$$

$$SO_4^{\bullet-} + OH^- \rightarrow SO_4^{2-} + HO^{\bullet} \quad (3)$$

$$S_2O_8^{2-} + HO^{\bullet} \rightarrow S_2O_8^{\bullet-} + OH^- \quad (4)$$

$$SO_4^{2-} + HO^{\bullet} \rightarrow SO_4^{\bullet-} + OH^- \quad (5)$$

Sulfate anion radical has a longer life time ($3–4 \times 10^{-5}$ s) compared with hydroxyl radical (2×10^{-8} s), therefore, it may have more chance of reacting with organic pollutants [19,20]. In majority of the works related to the application of the UV/PS process, high amounts of PS (1,000–10,000 mg L^{-1}) have been used in treatments [2,8,10,20]. It is since the sulfate ion is rather an environmentally low-risk ion. There is a maximum allowed concentration of 250 mg L^{-1} as a secondary drinking water standard, based on the taste of water, announced by the United States Environmental Protection Agency [21]. Also, the Water Corporation in Western Australia has approved the sulphate ion industrial waste discharge to environment of up to 600 mg L^{-1} [22].

Adding to this advantage, transition metals and especially ferrous metals, have been proven to be efficient PS activators [20]. The most frequently used transition metal is ferrous ion (Fe^{2+}) because of its low cost, easy availability, and high efficiency [23]. Moreover, iron salts can remove or reduce the solution turbidity because of the excellent coagulation ability of iron hydroxides [24,25].

Ferrous ions can rapidly activate PS to form sulfate radicals at a high rate (k = 27 M^{-1} s^{-1}) in the reaction [26]

$$S_2O_8^{2-} + Fe^{2+} \rightarrow Fe^{3+} + SO_4^{2-} + SO_4^{\bullet-} \quad (6)$$

On the other hand, excessive amounts of ferrous ion, may initiate a not favorable, scavenging reaction with sulfate radicals producing ferric compounds ($k = 4.6 \times 10^9$ M^{-1} s^{-1}), i.e. rapid conversion of Fe^{2+} to Fe^{3+} via [14,26]:

$$SO_4^{\bullet-} + Fe^{2+} \rightarrow Fe^{3+} + SO_4^{2-} \quad (7)$$

Accordingly, ferrous ions are converted simultaneously by both the PS ion and sulfate radicals and the final reaction product (SO_4^{2-}) remains in the system [14]. Therefore, PS activation using Fe^{2+} may be limited through PS radical scavenging when excessive Fe^{2+} is used.

This paper reports studies on degradation of organic pollutants in a real refinery wastewater, picked up from a point prior to entering the biological treatment unit. The homogeneous UV/PS/Fe^{2+} and other relevant alternative processes were used for this aim. One important advantage of homogenous processes is no requirement for separating solid adsorbents or catalyst powders, followed by their regeneration and reuse. To the best of our knowledge, no work has been reported dealing with the treatment of real refinery wastewater by different homogeneous UV/PS/Fe^{2+} processes.

2. Experimental

2.1. Chemicals and analysis methods

The refinery wastewater samples were collected from the wastewater leaving the dissolved air flotation (DAF) unit and entering the biological treatment unit in the Arak petroleum refinery plant. The COD of samples was within the range of 210–280 mg L^{-1}. Other specifications were pH: 7–8, turbidity: 90–120 NTU, total dissolved solids: 420–750 mg L^{-1}, biochemical oxygen demand (BOD): 70–95 mg L^{-1} and total suspended solids: 45–55 mg L^{-1}.

All chemicals were used as received without further purification. PS reagent is conventionally used in ammonium, sodium or potassium salts. Potassium salt was used here, due to reported better results in photo oxidative removal of some organic materials compared with other PS salts [10,17]. $K_2S_2O_3$ (99%) and $FeSO_4 \cdot 7H_2O$ (99.5%), for supplying Fe^{2+} ion were Merck (Germany) products. Sulfuric acid and sodium hydroxide solutions were used to adjust the pH of wastewater samples.

COD measurements were performed by the standard closed reflux and colorimetric method [27] using a COD reactor (HACH, DRB200) and a spectrophotometer (HACH, DR/2800) with the corresponding reagent. The turbidity of samples was scrutinized using a turbidimeter (Aqualytic AL250T-IR). The TOC of samples was also measured by means of a TOC analyzer (Shimadzu, VCSH model). The standard 5-d, BOD_5 test was used to assess reduction in BOD. Samples were stored at <4°C for approximately 24 h. Sample volumes ranging from 15 to 30 mL were brought to room temperature, placed in standard BOD bottles and filled with water buffered with a 1.0 mL L^{-1} phosphate buffer solution containing $MgSO_4$, $CaCl_2$, and $FeCl_3$ [27]. Samples were incubated at 20°C in a BOD incubator. The dissolved oxygen content was determined at inoculation and used after 5 d of incubation.

2.2. Reactor set-up and procedure

Experiments were conducted in a stainless steel rectangular cubic reactor (Fig. 1). The interior dimensions were 23 cm length, 7 cm width, and 21 cm depth. The reactor volume containing samples was about 1 L and the solution level was about 2 cm below the horizontal quartz tube inside

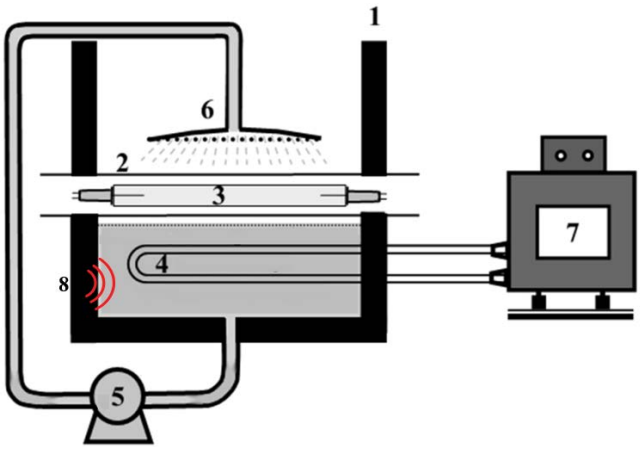

Fig. 1. The used photo-reactor setup; (1) reactor, (2) quartz tube, (3) UV lamp, (4) temperature regulating coil, (5) pump, (6) distributor, (7) thermostat, and (8) ultrasound source.

which the UV lamp was installed. The light source was a UV-C (Philips (Poland), TUV, 6 W) which was located horizontally in a quartz tube (2.5 cm diameter) at the center of the reactor. A pump circulated the content of the reactor so that the solution was sprayed over the quartz tube via a liquid distributor. Thus, a thin film of aqueous solution was formed around the quartz tube perimeter where the most degradation occurs in this region with the low mass transfer resistance. The solution was circulated, after facing the temperature adjustment coil. The device therefore facilitated the solution to expose the light in each circulation path. The reactor temperature was adjusted with an external water stream of a thermostat through the reactor coil. All experiments were conducted at 25°C except where stated for investigating temperature effect. For generating US waves (28 and 40 kHz, 50 W), a generator and a transducer (PARSONIC) were located outside adjacent to the reactor. Data at different conditions were obtained and analyzed using the COD removal criterion as:

$$\text{COD removal}(\%) = \frac{[\text{COD}]_0 - [\text{COD}]_t}{[\text{COD}]_0} \times 100 \quad (8)$$

where $[\text{COD}]_0$ and $[\text{COD}]_t$ are the appropriate initial and at any time t values.

2.2. Design of experiments

There is a multiplicity in the influencing factors as well as their interactions in AOPs. A conventionally used method is response surface methodology (RSM), which is able to optimize the operational factors and construct a descriptive mathematical model for the process [28]. In this work, optimization of the factors was performed by central composite design (CCD) as the most commonly used RSM methodology. The important operating factors of $K_2S_2O_3$ and $FeSO_4 \cdot 7H_2O$ dosages and pH were considered and COD removal of the wastewater was the response factor in the experimental design. A number of preliminary experiments were conducted to determine the range of the variables. Each of the variables was altered at five different levels ($-\alpha$, −1, 0, +1, $+\alpha$) and all of the variables were taken at a central coded value (denoted as zero level). Table 1 lists the level and range of the considered parameters as well as the designed CCD matrix which consists of three experimental points: cubic, axial and center points. The total number of required tests N can be determined from $N = 2^m + 2m + N_0$, where m is the number of factors 2^m and 2m and N_0 refer to the cubic, axial and the center point runs, respectively. In 2^m cubic experiments, all parameters are changed, allowing the study of the interaction between parameters from the obtained results. In 2m axial experiments, one parameter is at the highest and lowest limits i.e. ($+\alpha$) and ($-\alpha$) and the other parameters are fixed in the central point conditions. The last center duplicate experiments N_0 are designed to consider the experimental systematic errors. The distance of the axial points from the center points depends on the number of factors chosen for the experiments. The obtained COD removal values for corresponding experiments are listed in Table 1. The reaction time, in all the experiments, was limited to 60 min.

Table 1
The range and levels of variables and CCD matrix of experimental runs

Parameter	levels and ranges				
	$-\alpha$	low (–1)	middle (0)	high (+1)	$+\alpha$
$[K_2S_2O_8]$ (mg L^{-1})	100	201.3	350	498.6	600
$[FeSO_4 \cdot 7H_2O]$ (mg L^{-1})	2	7.7	16	24.3	30
pH	3	4.8	7.5	10.1	12

Design matrix				
Run	$[K_2S_2O_8]$ (mg L^{-1})	$[FeSO_4 \cdot 7H_2O]$ (mg L^{-1})	pH	COD removal (%)
1	600.00	16.00	7.50	32.18
2	498.65	7.68	4.82	30.14
3	350.00	16.00	7.50	51.9
4	350.00	16.00	7.50	53.6
5	350.00	30.00	7.50	44.12
6	350.00	16.00	3.00	59.18
7	498.65	24.32	10.18	25.11
8	350.00	16.00	7.50	56.7
9	498.65	24.32	4.82	54.17
10	350.00	16.00	7.50	58.19
11	201.35	7.68	4.82	39.9
12	201.35	24.32	10.18	34.15
13	350.00	16.00	7.50	56.12
14	350.00	16.00	7.50	54.17
15	498.65	7.68	10.18	26.17
16	350.00	16.00	12.00	24.8
17	100.00	16.00	7.50	43.17
18	350.00	2.00	7.50	25.21
19	201.35	24.32	4.82	65.18
20	201.35	7.68	10.18	32.25

3. Results and discussion

3.1. Operational parameters and the process optimization

The influence of the considered parameters on the UV/PS/Fe^{2+} process was presented by 3-D surface graphs in which the effects of two parameters were surveyed whereas the third one was maintained constant.

The results presented in Fig. 2 show that by increasing PS, up to about 302 mg L^{-1}, the COD removal increases as a consequence of more reactive radical generation. However, as reported in previous studies [17,29], increasing PS does not continuously improve the pollutants removal since PS itself behaves as a scavenger of $SO_4^{\bullet-}$ at elevated concentrations via:

$$S_2O_8^{2-} + SO_4^{\bullet-} \rightarrow SO_4^{2-} + S_2O_8^{\bullet-} \quad (9)$$

Fig. 2 also shows that by adding ferrous salt up to about 20 mg L^{-1}, COD removal is increased and after that a reduction is corresponding. As was pointed above, excess amounts of Fe^{2+} can lead to scavenging sulfate radicals and diminishing the process efficiency.

The influence of pH and PS dosages is presented in Fig. 3. As presented, COD removal reaches a maximum value at pH about 4.8 and decreases at either higher or lower pHs. Similar trends of variation have been previously reported for pollutants degradation by activated PS [9,29]. Under alkaline conditions, $SO_4^{\bullet-}$ species undergo reactions with OH^- to generate $HO^\bullet$ radicals according to Eq. 3. Despite conversion of $SO_4^{\bullet-}$ to SO_4^{2-} and producing $HO^\bullet$ radicals with the redox potential of 2.8 V that is slightly more than redox potential of $SO_4^{\bullet-}$ (2.5–3.1 V); extra amounts of SO_4^{2-} may act as $HO^\bullet$ radical scavenger [Eq. 5]. On the other hand, applying acidic conditions leads to additional $SO_4^{\bullet-}$ anion radical generation, according to the following equations [29]:

$$S_2O_8^{2-} + H^+ \rightarrow HS_2O_8^- \quad (10)$$

$$HS_2O_8^- \rightarrow SO_4^{\bullet-} + SO_4^{2-} + H^+ \quad (11)$$

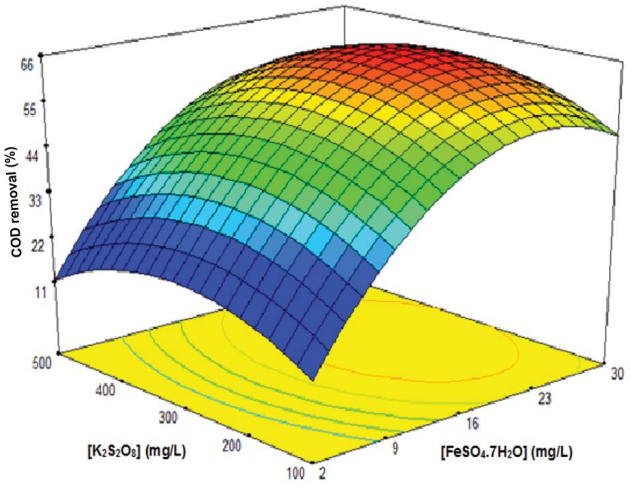

Fig. 2. Variation of COD removal as a function of $K_2S_2O_8$ and $FeSO_4.7H_2O$ concentrations for UV/PS/Fe^{2+} process; pH 4.8.

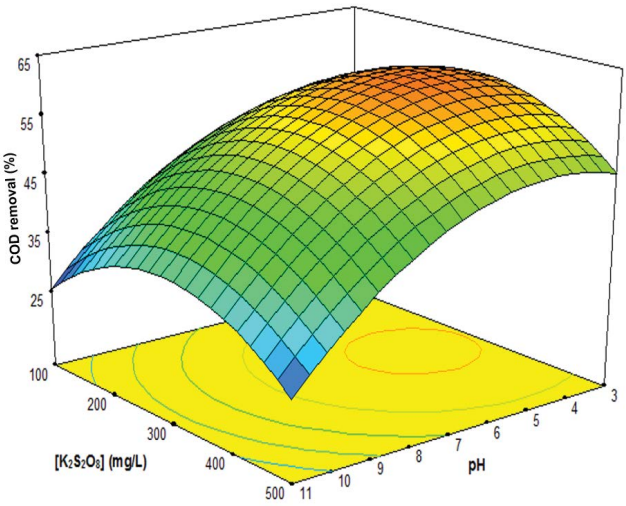

Fig. 3. Variation of COD removal as a function of pH and $K_2S_2O_8$ concentration for UV/PS/Fe^{2+} process; $[FeSO_4.7H_2O]$ = 20.3 mg L^{-1}.

Considering the highest level of degradation, obtained at pH 4.8, this amount can be considered as the optimum value.

Based on regression analysis, the provided data can be represented by a quadratic equation as

$$\text{COD removal}(\%) = 55.07 + 6.0\left[K_2S_2O_8\right] - 3.98\left[FeSO_4 \cdot 7H_2O\right] - 9.48\text{pH} - 6.06\left[K_2S_2O_8\right] \times \text{pH} + 6.95\left[K_2S_2O_8\right]^2 - 5.89\left[FeSO_4 \cdot 7H_2O\right]^2 - 4.36\text{pH}^2 \quad (12)$$

for which Table 2 lists the statistical criteria from the obtained data. A "Prob > *F*" value (*p*-value) less than 0.05 implies that a model term is significant and a value greater than 0.10 indicates a non-significant term. The model *F*-value of 118.87 and the *p*-value of less than 0.0001 indicate that the model is significant and the "Lack-of-Fit of *F*-value" of 0.64 is corresponding [28,30]. The adequacy of the model was also examined by software and residuals are demonstrated by Fig. 4. The residuals show that points are adopting a straight line trend. The closer the data to the straight line, the better is the data distribution in the scales demonstrated.

Apart from these criteria, the model feature can be seen in Fig. 5, indicating a good agreement between the experimental and predicted values. Further, the overall performance of the model can be assessed by the coefficient of determination (R^2), as the degree of closeness between the observed and predicted COD removals. For this model, R^2 value of 0.985 confirms that the model is satisfactory. The Pareto graph showed that the effect of pH was more than the other parameters.

The optimized operating parameters, based on the objective of maximizing COD removal, were determined. A maximum value of 65.6% was predicted for this process under optimum conditions of $[K_2S_2O_3]$ = 302.9 mg L^{-1}, $[FeSO_4 \cdot 7H_2O]$ = 20.3 mg L^{-1} and pH = 4.8. Meanwhile, confirmatory experimental runs under these conditions, indicated a COD removal of 66.6% after 60 min. This close agreement confirms the model validity.

Table 2
Statistical criteria, ANOVA and lack-of-fit tests for the response quadratic Eq. 12

Source	Sum of squares	Degree of freedom	Mean square	*F* Value	Prob > *F*	Remarks
Model	3,471.55	7	495.94	118.87	<0.0001	Significant
$[K_2S_2O_8]$	216.48	1	216.48	51.89	<0.0001	
$[FeSO_4 \cdot 7H_2O]$	491.79	1	491.79	117.88	<0.0001	
pH	1,228.54	1	1,228.54	294.48	<0.0001	
pH × $[FeSO_4 \cdot 7H_2O]$	293.67	1	293.67	70.39	<0.0001	
$[K_2S_2O_8]^2$	499.95	1	499.95	119.84	<0.0001	
$[FeSO_4 \cdot 7H_2O]^2$	696.93	1	696.93	167.05	<0.0001	
pH^2	274.50	1	274.50	65.80	<0.0001	
Residual	50.06	12	4.17			
Lack of Fit	23.56	7	3.37	0.64	0.7181	non-significant
Pure error	26.50	5	5.30			
Cor total	3,521.61	19				

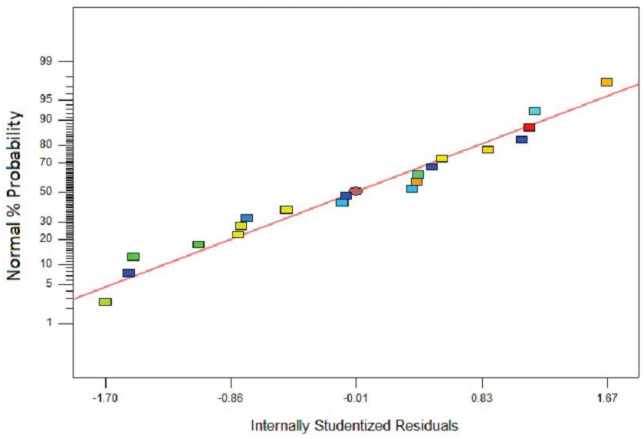

Fig. 4. Diagram of normal plot of studentized residuals for COD removals.

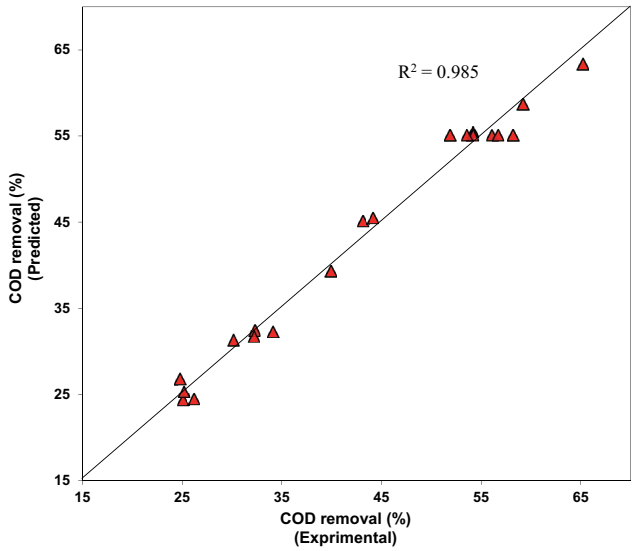

Fig. 5. The model predicted COD removal versus its experimental values for UV/PS/Fe^{2+} process.

The BOD_5/COD ratio of wastewater was initially within 0.30–0.48. The COD and BOD_5 measurements of the wastewater were reduced respectively to 93 and 49 mg L^{-1} after treatment under optimum conditions. Therefore, BOD_5/COD values after UV/PS/Fe^{2+} process was increased to 0.49–0.63. It has been reported that a wastewater with BOD_5/COD value of more than 0.4 can be considered for biodegradation [7], confirming capability of biodegradation of materials, compared with mother compounds. Here, the refinery wastewater samples were collected from the wastewater leaving the DAF unit and while entering the biological treatment. Therefore, the UV/PS/Fe^{2+} process provides an advancement in the treatment of real petroleum wastewater, using a rather low cost AOP process.

In addition, performing TOC and turbidity analysis under optimum conditions revealed 39.2% and 76.9% removals after 60 min (Fig. 6). Thus, process efficiency based on TOC criterion was found lower than the corresponding COD, indicating a part of recalcitrant organic compounds in the samples as expected. The reduction in turbidity can be attributed to the degradation of organic compounds and their mineralization [31] as well as the coagulation due to the presence of iron salts. The study by Li et. al. [25], for instance, shows that the coagulation ability of the colloidal ferric hydroxide produced by the Fe^{2+}, could further improve the pollution removal in wastewater, coupled with the oxidability of PS.

3.2. *Effects of US waves and heating*

Experiments were conducted under optimum conditions while 28 and 40 kHz US waves were irradiated. When UV/PS/Fe^{2+} process was assisted with the US, the efficiency was improved to 78.5% with 40 kHz and to 70.3% with 28 kHz waves (Fig. 7). The enhancement potentially occurs because US accelerates the activation of PS to produce $SO_4^{\bullet-}$, which further captures hydrogen atoms from water to form $HO^{\bullet}$ radical [32,33]:

$$S_2O_8^{2-} \xrightarrow{)))} 2SO_4^{\bullet-} \quad (13)$$

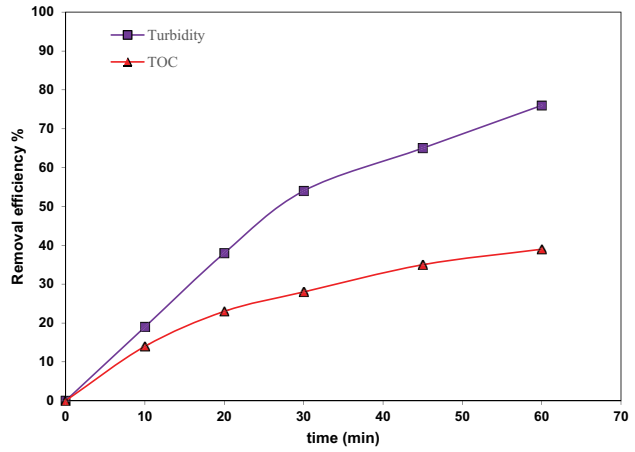

Fig. 6. Removal efficiency based on turbidity and TOC for UV/PS/Fe^{2+} process under optimum conditions.

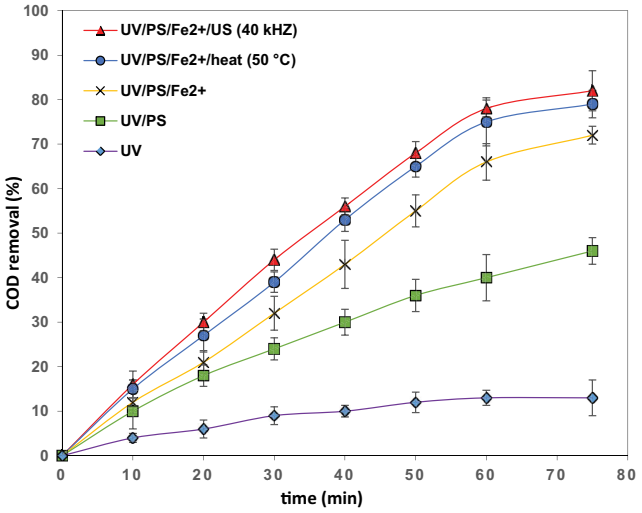

Fig. 7. Variation of COD removal with time for different processes under optimum conditions.

$$SO_4^{\bullet-} + H_2O \rightarrow HSO_4^- + HO^{\bullet} \quad (14)$$

where symbol ")))" denotes US waves.

Moreover, to study heat effect, experiments were conducted at different temperatures under optimum other conditions. The favorite influence of temperature was observed. Increasing temperature, from the so far dominant temperature of 25°C–50°C, increased the COD removal from 66.6% to 75.9%. Under these conditions, heat activation of PS ions assists the US reaction similar to Eq. 13.

For proper evaluations, different alternatives of the considered process were examined. Based on the obtained COD removals, as presented in Fig. 7; the used processes were efficient in the order of: UV/PS/Fe^{2+}/US > UV/PS/Fe^{2+}/heat > UV/PS/Fe^{2+} > UV/PS > UV. Apparently, UV light alone, with no PS, had no sensible influence with respect to the low power UV lamp. It was while using PS significantly improved the efficiency and that further assisting by ferrous ions enhanced the process performance to a high extent.

3.3. The rate of COD removal

With respect to practical applications, the rate of COD removal for the UV/PS/Fe^{2+} process under the optimum conditions was investigated. Fig. 8 shows that the results agree well with an overall pseudo first order model as:

$$\ln\frac{[\mathrm{COD}]_0}{[\mathrm{COD}]_t} = k \times t \quad (15)$$

where $[COD]_0$ and $[COD]_t$ are the appropriate initial and at any time values. The coefficient of determination (R^2) was 0.997. Thus, a pseudo first order reaction can be attributed to the COD removal of the refinery wastewater under the optimum conditions. The appropriate overall rate constant was 0.0218 min^{-1}.

3.4. Energy consumption estimation

The cost effectiveness is essential among several criteria considered for the selection or evaluation of different wastewater treatment methods. Accordingly, the total operating cost was considered as the sum of the major imposed costs of electrical energy of the light irradiation (E_{EC}) and the used chemicals [2,34].

In a photochemical process, the electrical energy consumption (in kWh m^{-3}) for one order of magnitude degradation, can be calculated by the equation recommended by the photochemistry commission of the international union of pure and applied chemistry (IUPAC) as [34,35]:

$$E_{EC} = \frac{1{,}000 \times p \times t}{60V \log\frac{[\mathrm{COD}]_0}{[\mathrm{COD}]_t}} \quad (16)$$

where P is the electric power (in kW) of the photochemical system used for light source, V is the volume (L) of the treated solution and t is the treatment time (in min).

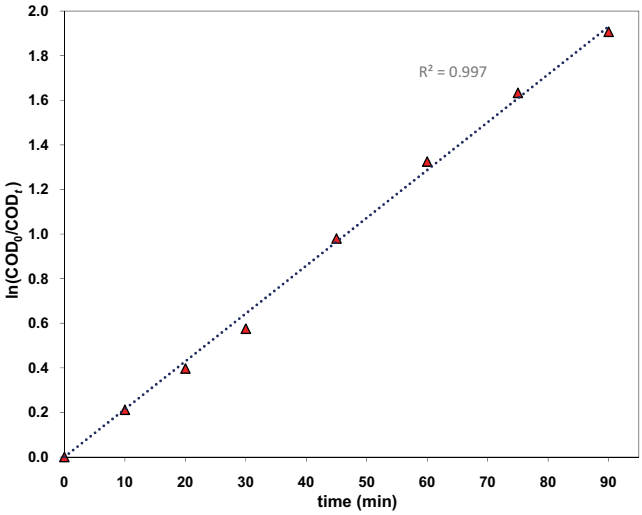

Fig. 8. The diagram of the rate of COD removal for UV/PS/Fe^{2+} process under optimum conditions.

Since a pseudo first-order reaction was found here; $\ln([COD]_0/[COD]_t)/t$ represents the rate constant, k (in min^{-1}). The simplified following formula can therefore be used:

$$E_{EC} = \frac{38.4 \times p}{V \times k} \tag{17}$$

Accordingly, electrical energy consumption for one order of magnitude COD removal, under optimal conditions, was obtained as 10.56 kWh (per cubic meter of wastewater). Given the electrical energy cost in U.S. market as \$0.129 kWh^{-1} in 2018 [36], the energy cost is obtained \$1.36 m^{-3} for the used process. By adding the price of the required chemicals, i.e. $K_2S_2O_3$ (1.5 \$ kg^{-1}) and $FeSO_4.7H_2O$ (\$0.2 kg^{-1}) [37] to the electrical energy costs, total operating cost obtained as \$1.82 m^{-3}. Our previous investigation [38] indicated a much higher energy cost for treatment of real refinery wastewater by UV/TiO_2 heterogeneous process.

4. Conclusions

The aim of this work was to evaluate the performance of using environmental friendly PS and ferrous ions in the homogenous photochemical treatment of petroleum refinery wastewater and evaluating the influence of operating parameters. Results showed that operations under PS concentration of 302.9 mg L^{-1}, ferrous salt concentration of 20.3 mg L^{-1} and pH 4.8 could significantly reduce the COD, turbidity and TOC to 66.6%, 76.9%, and 39.2% respectively after 60 min. Meanwhile, utilizing US and increasing temperature revealed significant positive effects in the process. A first-order COD removal rate was determined under optimal conditions, and accordingly, electrical energy consumption for one order of magnitude COD removal as well as the total operating cost were estimated to be quite low.

Acknowledgment

The authors wish to acknowledge the financial support by the Arak petroleum refinery company.

References

[1] L.W. Matzek, K.E. Carter, Activated persulfate for organic chemical degradation: a review, Chemosphere, 151 (2016) 178–188.
[2] J. Saien, M. Moradi, A.R. Soleymani, Homogenous persulfate and periodate photochemical treatment of furfural in aqueous solutions, CLEAN – Soil Air Water, 45 (2017) 1–8.
[3] A. Seid-Mohammadi, G. Asgari, A. Poormohammadi, M. Ahmadian, H. Rezaeivahidian, Removal of phenol at high concentrations using UV/Persulfate from saline wastewater, Desal. Wat. Treat., 57 (2016) 19988–19995.
[4] S. Wacławek, H.V. Lutze, K. Grübel, V.V. Padil, M. Černík, D.D. Dionysiou, Chemistry of persulfates in water and wastewater treatment: a review, Chem. Eng. J., 330 (2017) 44–62.
[5] A. Kambhu, S. Comrort, C. Chokejaroenart, C. Sakulthaew, Developing slow-release persulfate candles to treat BTEX contaminated groundwater, Chemosphere, 89 (2012) 656–664.
[6] K. Kaur, M. Crimi, Release of chromium from soils with persulfate chemical oxidation, Ground Water, 52 (2014) 748–755.
[7] A.A. Babaei, F. Ghanbari, COD removal from petrochemical wastewater by UV/hydrogen peroxide, UV/persulfate and UV/percarbonate: biodegradability improvement and cost evaluation, J. Water Reuse Desal. 6 (2016) 484–494.
[8] F. Ghanbari, M. Moradi, Application of peroxymonosulfate and its activation methods for degradation of environmental organic pollutants: review, Chem. Eng. J., 310 (2017) 41–62.
[9] K.C. Huang, R.A. Couttene, G.E. Hoag, Kinetics of heat-assisted persulfate oxidation of methyl tert-butyl ether (MTBE), Chemosphere, 49 (2002) 413–420.
[10] J. Saien, A.R. Soleymani, J. Sun, Parametric optimization of individual and hybridized AOPs of Fe^{2+}/H_2O_2 and $UV/S_2O_8^{2-}$ for rapid dye destruction in aqueous media, Desalination, 279 (2011) 298–305.
[11] Q. Zhao, Q. Mao, Y. Zhou, J. Wei, X. Liu, J. Yang, L. Luo, J. Zhang, H. Chen, L. Tang, Metal-free carbon materials-catalyzed sulfate radical-based advanced oxidation processes: a review on heterogeneous catalysts and applications, Chemosphere, 189 (2017) 224–238.
[12] C. Liang, Y.Y. Guo, Y.C. Chien, Y.J. Wu, Oxidative degradation of MTBE by pyrite-activated persulfate: proposed reaction pathways, Ind. Eng. Chem. Res., 49 (2010) 8858–8864.
[13] J. Criquet, N.V. Leitner, Electron beam irradiation of aqueous solution of persulfate ions, Chem. Eng. J., 169 (2011) 258–262.
[14] C. Liu, K. Shih, C. Sun, F. Wang, Oxidative degradation of propachlor by ferrous and copper ion activated persulfate, Sci. Total Environ., 416 (2012) 507–512.
[15] R. Xu, X. Li, Degradation of azo dye Orange G in aqueous solutions by persulfate with ferrous ion, Sep. Purif. Technol., 72 (2010) 105–111.
[16] Y. Deng, R. Zhao, Advanced oxidation processes (AOPs) in wastewater treatment, Curr. Pollut. Rep., 1 (2015) 167–176.
[17] D. Salari, A. Niaei, S. Aber, M.H. Rasoulifard, The photooxidative destruction of CI Basic Yellow 2 using $UV/S_2O_8^{2-}$ process in a rectangular continuous photoreactor, J. Hazard. Mater., 166 (2009) 61–66.
[18] T.K. Lau, W. Chu, N.J. Graham, The aqueous degradation of butylated hydroxyanisole by $UV/S_2O_8^{2-}$: study of reaction mechanisms via dimerization and mineralization, Environ. Sci. Technol., 41 (2007) 613–619.
[19] F. Ghanbari, M. Moradi, F. Gohari, Degradation of 2, 4, 6-trichlorophenol in aqueous solutions using peroxymonosulfate/activated carbon/UV process via sulfate and hydroxyl radicals, J. Water Process Eng., 9 (2016) 22–28.
[20] A.R. Soleymani, M. Moradi, Performance and modeling of UV/persulfate/Ce(IV) process as a dual oxidant photochemical treatment system: kinetic study and operating cost estimation, Chem. Eng. J., 347 (2018) 243–251.
[21] E. Weiner, A dictionary of inorganic water quality parameters and pollutants, Applications of Environmental Chemistry: A Practical Guide for Environmental Professionals , CRC Press, Boca Raton, FL, 27 (2000).
[22] Water Corporation (2003), Detailed acceptance criteria, publication No. IWPUB 06, June 2003, Australia.
[23] S. Yan, W. Xiong, S. Xing, Y. Shao, R. Guo, H. Zhang, Oxidation of organic contaminant in a self-driven electro/natural maghemite/peroxydisulfate system: efficiency and mechanism, Sci. Total Environ., 5999 (2017) 1181–1190.
[24] S.M. Ponder, J.G. Darab, T.E. Mallouk, Remediation of Cr(VI) and Pb(II) aqueous solutions using supported, nanoscale zero-valent iron, Environ. Sci. Technol., 34 (2000) 2564–2569.
[25] K. Li, H. Li, T. Xiao, G. Zhang, J. Long, D. Luo, Q. Wang, Removal of thallium from wastewater by a combination of persulfate oxidation and iron coagulation, Process Saf. Environ. Prot., 119 (2018) 340–349.
[26] C. Liang, H.W. Su, Identification of sulfate and hydroxyl radicals in thermally activated persulfate, Ind. Eng. Chem. Res., 48 (2009) 5558–5562.
[27] A.D. Eaton, L.S. Clesceri, A.E. Greenberg, Standard Methods for the Examination of Water and Wastewater, American Public Health Association, Washington, DC, 1995.
[28] S. Dutta, A. Bhattacharyya, A. Ganguly, S. Gupta, S. Basu, Application of response surface methodology for preparation

of low-cost adsorbent from citrus fruit peel and for removal of methylene blue, Desalination, 275 (2011) 26–36.
[29] A.R. Soleymani, J. Saien, H. Bayat, Artificial neural networks developed for prediction of dye decolorization efficiency with UV/$K_2S_2O_8$ process, Chem. Eng. J., 170 (2011) 29–35.
[30] P. Sharma, L. Singh, N. Dilbaghi, Response surface methodological approach for the decolorization of simulated dye effluent using Aspergillus fumigatus fresenius, J. Hazard. Mater., 161 (2009) 1081–1086.
[31] S. Tripathi, S.V. Pathak, D.M. Tripathi, B.D. Tripathi, Application of ozone based treatments of secondary effluents, Bioresour. Technol., 102 (2011) 2481–2486.
[32] G.J. Price, A.A. Clifton, F. Keen, Ultrasonically enhanced persulfate oxidation of polyethylene surfaces, Polymer, 37 (1996) 5825–5829.
[33] Q. Yang, Y. Zhong, H. Zhong, X. Li, W. Du, X. Li, R. Chen, G. Zeng, A novel pretreatment process of mature landfill leachate with ultrasonic activated persulfate: optimization using integrated Taguchi method and response surface methodology, Process Saf. Environ. Prot., 98 (2015) 268–275.
[34] J. Saien, A. Azizi, Simultaneous photocatalytic treatment of Cr(VI), Ni(II) and SDBS in aqeuous solutions: evaluation of removal efficiency and energy consumption, Process Saf. Environ. Prot., 95 (2015) 114–125.
[35] J.R. Bolton, K.G. Bircher, W. Tumas, C.A. Tolman, Figures-of-merit for the technical development and application of advanced oxidation technologies for both electric-and solar-driven systems, Pure Appl. Chem., 73 (2001) 627–637.
[36] US Energy Information Administration (EIA), Independent Statistics and Analysis, US Department of Energy, Washington, DC, 20585, 2018.
[37] http://www.alibaba.com, accessed 2018
[38] J. Saien, H. Nejati, Enhanced photocatalytic degradation of pollutants in petroleum refinery wastewater under mild conditions, J. Hazard. Mater., 148 (2007) 491–495.